# Stiffness Mapping in Biological Materials based on MRI Imaging and Topology Optimization

L. Cai [1], C. Pedersen [2], R. Mclendon [2], M. Biedermann [2], G. Dimitrova [2], J. Yao [2], C.P. Neu [3]

1. Biomedical Engineering Department, Purdue University, West Lafayette, IN, US

2. Dassault Systèmes, Johnston, RI, US

3. Mechanical Engineering Department, University of Colorado, Boulder, CO, US

**Abstract**: *Magnetic resonance imaging (MRI) is a preeminent technology to visualize the internal tissue structure, in addition to other physical phenomena like flow and diffusion. One specialized MRI technique, termed displacements under applied loading by MRI (dualMRI), was developed to measure displacements and strain in musculoskeletal tissues, hydrogels, and engineered constructs. However, deformation information does not directly describe spatial distributions of tissue stiffness, which is critical to the understanding of disease progression. In order to achieve this goal, here we proposed an inverse modeling approach based on Tosca and Abaqus to map the internal stiffness nondestructively from image-based displacements measured in different biological constructs. In this study, the inverse simulation was validated on displacements results derived from forward simulations where materials properties and boundary conditions were known. With different level of noise added, the error associated with the relative stiffness mapping technique was studied and the optimized smoothing technique was chosen. To analyze the effects of each parameter in the inverse modeling process, sensitivity analysis was done using Cotter's method. Additionally, experimental data from bi-layered agarose gel under different loading conditions were modeled, with plane stress assumption in two dimensions. The significance and potential of this approach was highlighted for the description of tissue degeneration, repair, and complex material properties.*

***Keywords****: Inverse Modeling, magnetic Resonance Imaging (MRI), Abaqus, Tosca, stiffness, cartilage*

## 1. Introduction

Nondestructive visualization and quantification on in vivo anatomy and physiology has always been a goal of biomedical engineering. For tissue scale studies, joint can be scanned in vivo for tissue morphology using Magnetic resonance imaging (MRI) or computed tomography, coupled with other techniques to measure load response of tissue. However, few noninvasive techniques are designed to be able to measure internal mechanical behavior, which vary by location and scale. Magnetic resonance elastography (MRE) can be used to estimate the stiffness of softer tissue

under high frequency loading, however, the large dissipation of waves in human body, especially in stiff cartilage, restricts MRE to ex vivo applications (Hardy, 2005; Lopez, 2008). Mathematical models of joint biomechanics were also used with morphologic imaging to determine internal tissue mechanical behavior. However, material properties are usually unknown and assumptions are made to estimate the internal deformations (Bingham, 2008; Li, 2001). One specialized MRI technique, termed displacements under applied loading by MRI (dualMRI), was developed to measure displacements and strain in musculoskeletal tissues, hydrogels, and engineered constructs (Chan, 2012). However, displacement and strain information alone does not directly describe spatial distributions of tissue stiffness, which is critical to the understanding of disease progression (Kempson, 1971) (Neu, 2014). In order to achieve stiffness mapping nondestructively in explanted tissues or even in living animals or humans *in vivo*, we need to use an inverse modeling approach based on image-based displacements. The relative stiffness can be reconstructed from the displacement by either direct or iterative methods, between which the iterative method was found to be more robust (Oberai, 2003). However, it usually requires a regularization term and the value of this regularization parameter has significant effects on the reconstructed results (Richards, 2009). Besides, the intense calculation process requires a lot of computer memory and time, and can be cumbersome (Zhu, 2003). To avoid these disadvantages, we proposed a method using the Abaqus optimization suite Tosca to do the inverse modeling.

## 2. Methods

In the present study, topology optimization, which is usually used to design stiff, durable and light-weight structures, was applied to determine the stiffness distribution of agarose materials. Specifically, the design variable was the elemental relative density ($\rho$) of each individual finite element in the design space. The elastic modulus of the element was described as $E = \rho E_0$, where E and $E_0$ were the moduli for the current model and the base model respectively. Other than traditional topology optimizations, which use Solid Isotropic Material with Penalization (SIMP) or Rational Approximation of Material Properties (RAMP), the current work is designed to minimize the maximum absolute difference of the displacement (U) at N discrete points between the simulation and the experimental measurements:

$$Min : Max_{i=1}^{N} \left( \left| U_{\exp}(P_i) - U_{sim}(P_i) \right| \right) \quad (1)$$

The optimization formulation was solved using an iterative design. In each iteration, the equilibrium of the model was determined using Abaqus (V6.14-5, Dassault Systèmes), and the sensitivities with respect to the elemental relative densities were computed for the objective function and constraints analytically (Abaqus Users manual, 2014; Bendsoe, 2003). The elemental relative densities were updated along with the iteration until a stop criterion was satisfied.

In order to validate the approach, a forward simulation of a cylindrical model was created (Figure 1). To test whether our approach could differentiate between material regions of different stiffness, a simple bi-layer structure (Griebel, 2014) was introduced, with a higher modulus (E=10 *MPa*,

ν=0.49) in the bottom and lower modulus (E=5 *MPa*, ν=0.49) in the top. With the bottom edge of the model fully constrained, the top edge was indented to 15% of the thickness. Displacements of this loaded model were calculated by Abaqus and passed to Tosca (Dassault Systèmes) as design reference. To inversely calculate the stiffness map, optimization was initiated using a model with linear elastic (Young's modulus E=8 *MPa*) properties. The difference between displacements of a target and reference model was optimized (Equation 1). To evaluate the sensitivity and stability of the method, uniform symmetric random noise was added to the reference displacement data prior to optimization. Different noise levels in Figure 1 presents the ratio of the noise amplitude to the indentation depth. The included noise levels were 0, 0.05%, 1%, 10% and 50%.

To test the sensitivity of all the factors involved so that efforts will be more focused, Cotter's method (Cotter, 1979) was used. In this design, input parameters that may influence the output of the model were identified, with a low value and a high value considered for each parameter. The tested factors include noise level of the displacement input data, data smoothing, model elasticity, 2D assumption, boundary geometry, density move (the design variable update limit for each iteration), initial density and filter radius. It is to note that the last three factors are parameters used in Tosca to guide the convergence process. In this sensitivity test, the simulation was run once with all parameters were at their low value, once with all parameters at their high level, once with each parameter at high level while others at their low levels and once each parameter at low level while others at their high levels. At last, the impact of each factor was calculated by comparing the sensitivity factors calculated from the output biases.

The inverse modeling approach was further tested on experimental data of engineered agarose constructs (Griebel, 2014) (Figure 2). In the setup, two different layered agarose constructs of 2% and 4% w/v were prepared of cylindrical shape with a 10 *mm* diameter and 6 *mm* depth. The first layered agarose gel has a thickness ratio of 1:2 for 2% and 4% gels and the 2% gel was on top. For the second agarose gel, the thickness ratio is 2:1 for 2% and 4% gels, and on the opposite, the 4% gel was on top. The samples were cyclically loaded by a horizontally-oriented cylindrical indenter, and loading actions were synchronized with a 14.1 T MRI system (Bruker Medical GMBH), in which a dualMRI (DENSE-FISP) imaging sequence (Chan, 2012) with a displacement encoding gradient 2.13 $\pi$/*mm* was programed. The displacement data measured was reconstructed to the undeformed state, and then sampled evenly as the reference displacement. To simplify the problem, plane stress was assumed in the middle portion of the imaging section and a 2D model was created. Since the cyclic load was measured, it was feasible to scale the relative stiffness map to derive the real stiffness map by comparing the supporting force in the target model with the known load applied experimentally.

## 3. Results

The validation and stability study showed that the proposed inverse algorithm produced the original stiffness pattern and worked robustly within certain levels of applied noise. In the case of ideal (no noise) data (Figure 1A), the inverse modeling produced a distinctive bilayer configuration and the averaged stiffness ratio between two layers was 0.49997, which was very close to the original 0.5 setting. When 1% noise was introduced, the ratio became 0.54. Though

there were several out-of-range elements near the boundary, the bilayer configuration remained. For noise levels of 10% and 50%, the optimization process stopped at iteration number 5, while the other cases with less noise continue to converge toward zero (Figure 1B; iterations after 7 not shown). The relative stiffness for all noise levels showed a stiffer bottom layer (Figure 1C).

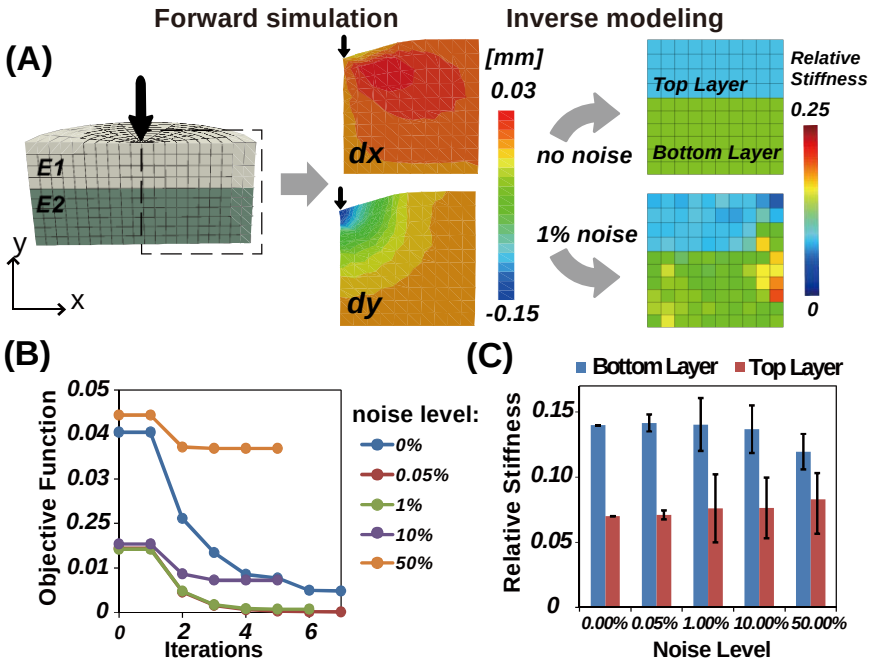


**FIGURE 1. Workflow of the inverse modeling by Tosca/Abaqus using the displacement data from forward simulation of a two layer cylinder (with E2=2×E1) (A). The relative stiffness result was presented for cases with and without added noise. The relationship between objective function value and iteration numbers (B). Averaged relative stiffness of top and bottom layer when different noise level was added (C).**

The Cotter's sensitivity analysis was listed in Table 1. The primary inputs to the inverse model were the displacement data and its geometry. They were both affected by the imaging noise and the smoothing process afterwards. As it can be seen from Table 1, the 2D assumption was the most important factor, which indicated the deficiency of the 2D assumption and the importance of the out-of-plane strains measurement. The inverse modeling was also sensitive to boundary

geometries, which indicated a need for more accurate method to draw region of interest. At last, the large effect of smoothing process showed it also needed a careful investigation, to make sure no bias was created.

**Table 1. Factor sensitivity calculated by Cotter's method**

| Facotrs | Factors Name | Low level | High level | Sensitivity Factor (%) |
|---|---|---|---|---|
| 1 | Noise level | 0 | Normally distributed ($\sigma$=20 $\mu m$) | 14.3 |
| 2 | Smoothing | 0 | 10 cycles Gaussian filter (kernel 3) | 10.5 |
| 3 | Elasticity | Linear elastic | Neo Hookean | 2.4 |
| 4 | 2D assumption | Plane Strain | Plain Stress | 39.8 |
| 5 | Boundary geometry | No bias | Edge location biased by random noise ($\sigma$=20 $\mu m$) | 15.9 |
| 6 | Density move | 0.1 | 0.05 | 8.0 |
| 7 | Initial density | 0.5 | 0.2 | 5.2 |
| 8 | Filter radius | 1.2e-9 *mm* | 1.2 *mm* | 4.0 |

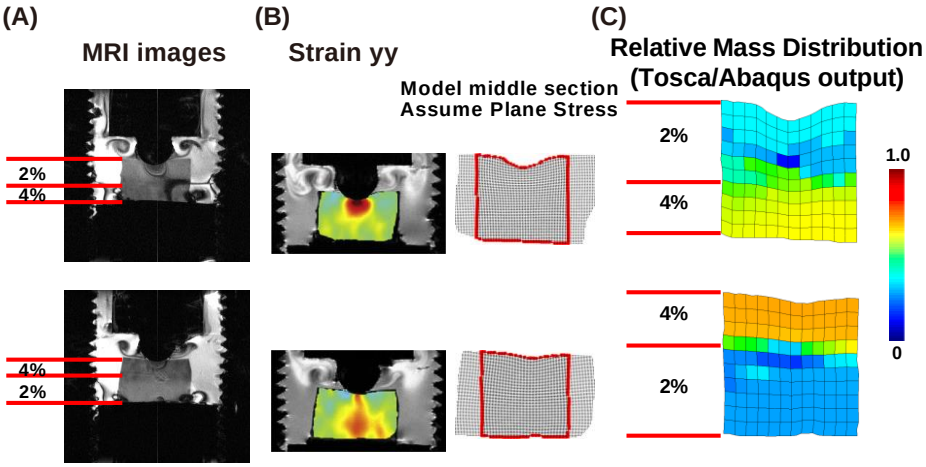


**FIGURE 2. Inverse modeling on bi-layer agarose. (A) MRI images of two types of bi-layer agarose gels. The first one had 2% (softer) gel at the top and 4% (stiffer) gel at the bottom with a thickness ratio of 2:1. The other one was 4% at the top and 2% at the bottom with a thickness ratio 1:2. (B) Strain yy for each gel type was shown for each case and the modeling part was marked red in the nodes map. (C) The relative mass distribution was shown as results of inverse modeling**

For the bi-layered agarose gel study, two types of gel were cyclically loaded and imaged in MRI (Figure 2A). In Figure 2B, the first gel showed that the strain yy was restricted in the top softer layer. However, it penetrated more to the bottom layer in the second gel since its top layer was stiffer compared to the bottom layer. To simplify this three dimension problem into two dimension, we assume that the loading is plane stress. In addition, the middle section data was extracted to build a model in Abaqus. The relative mass distribution in Figure 2C was the output of Tosca and has the same meaning of relative stiffness distribution. It can be seen that the bi-layers construction was distinct and fitted the real material.

## 4. Discussion

The results showed that combined deformation imaging and topology optimization is robust in the bilayer case but requires accurate input of boundary conditions. The boundary issues observed (Figure 1A, 2) might be related with the over-constricted boundary nodes, since they have smallest displacements and should be most sensitive to noise. It was also found that more complex stiffness patterns, like higher stiffness ratio between two layers, tends to slow down the convergence iterations, since it deviates more from the initial homogeneous model.

In the Cotter's method, the two dimensional assumption surprisingly made the greatest difference. This indicates that it is important to describe the out of plane displacement instead of simplifying it to be strain stress or strain plane. A three dimensional imaging would be helpful to solve this problem. Moreover, the noise level and its corresponding smoothing technique made a difference. Other two dimensional fittings will be studied further in the future. The boundary geometry was another important factor which indicated the necessity to use a more accurate automatic mask drawing algorithm.

The agarose gel used in Figure 2 has been tested in (Griebel, 2014). It showed that the 2% and 4% agarose gel has an instantaneous modulus ratio of 0.43 and an equilibrium modulus ratio 0.20. Since the 0.33 *Hz* quasi-steady state cyclic loading in this study can be treated as equilibrium condition (Neu, 2008), the value 0.20 under equilibrium condition should be used. As a comparison, the relative mass ratio between 2% and 4% in Figure 2C was calculated to be 0.5 for the first gel and 0.28 for the second gel. The first one diverged from 0.20 value which might be due to the plastic deformation caused by the cyclic loading. Homogeneous agarose cyclic loading test indicated that the loading region tended to become stiffer (data not shown). The same condition could has happened in the first gel as well.

## 5. Conclusions

In summary, our inverse modeling approach, which was built on the displacement-encoded MRI, provided more intuitive result of the stiffness distribution inside the tissue. The nondestructive nature and the various types of elemental type in Abaqus extended the potential application of this method. This approach may be useful to analyze softening observed in the timecourse of tissue degeneration, for example in diseases including osteoarthritis. It may also be possible to monitor repair success using stiffness mapping as a unique imaging biomarker for tissue function.

## 6. Acknowledgements

The authors would like to acknowledge funding from NIH R01 AR063712 and NSF CAREER 1349735.

## 7. References

**1.** Abaqus Users manual, Version 8.1.0, Dassault Systemes Simulia Corp., Providence, RI., 2014.

**2.** Bendsoe, Martin Philip, and Ole Sigmund, "Topology optimization: theory, methods and applications", Springer, 2003.

**3.** Bingham, JT, et al., "In vivo cartilage contact deformation in the healthy human tibiofemoral joint". Rheumatology 47(11), 1622-1627, 2008.

**4.** Chan, Deva D, and Corey P Neu, "Transient and microscale deformations and strains measured under exogenous loading by noninvasive magnetic resonance". PloS one 7(3), e33463, 2012.

**5.** Cotter, Sarah C, "A screening design for factorial experiments with interactions". Biometrika 66(2), 317-320, 1979.

**6.** Griebel, AJ, et al., "Direct noninvasive measurement and numerical modeling of depth-dependent strains in layered agarose constructs". Journal of biomechanics 47(9), 2149-2156, 2014.

**7.** Hardy, Peter A, et al., "Imaging articular cartilage under compression—cartilage elastography". Magnetic resonance in medicine 53(5), 1065-1073, 2005.

**8.** Kempson, GE, et al., "Patterns of cartilage stiffness on normal and degenerate human femoral heads". Journal of biomechanics 4(6), 597IN25609-608IN26, 1971.

**9.** Li, G., O. Lopez, and H. Rubash, "Variability of a three-dimensional finite element model constructed using magnetic resonance images of a knee for joint contact stress analysis". J Biomech Eng 123(4), 341-6, 2001.

**10.** Lopez, Orlando, et al., "Characterization of the dynamic shear properties of hyaline cartilage using high-frequency dynamic MR elastography". Magn Reson Med 59(2), 356-64, 2008.

**11.** Neu, Corey P, and Jeffrey H Walton, "Displacement encoding for the measurement of cartilage deformation". Magnetic Resonance in Medicine 59(1), 149-155, 2008.

**12.** Neu, CP, "Functional imaging in OA: role of imaging in the evaluation of tissue biomechanics". Osteoarthritis and Cartilage 22(10), 1349-1359, 2014.

**13.** Oberai, Assad A, Nachiket H Gokhale, and Gonzalo R Feijóo, "Solution of inverse problems in elasticity imaging using the adjoint method". Inverse Problems 19(2), 297, 2003.

**14.** Richards, Michael S, Paul E Barbone, and Assad A Oberai, "Quantitative three-dimensional elasticity imaging from quasi-static deformation: a phantom study". Physics in medicine and biology 54(3), 757, 2009.

**15.** Zhu, Yanning, Timothy J Hall, and Jingfeng Jiang, "A finite-element approach for Young's modulus reconstruction". Medical Imaging, IEEE Transactions on 22(7), 890-901, 2003.